

# Gas sensor based on graphene sheet derivatives decorated by Ni or As atoms

Alaa A. Al-Jobory<sup>1</sup>, Turki Alotaibi<sup>2</sup>, and Ali K. Ismael<sup>2</sup>

<sup>1</sup>Department of Physics, College of Science, University Of Anbar, Anbar, Iraq

<sup>2</sup>Department of Physics, Lancaster University, Lancaster LA1 4YB, UK.

[a.al-jobory@uoanbar.edu.iq](mailto:a.al-jobory@uoanbar.edu.iq)

## Abstract

The current study selectivity tunes the graphene derivatives' ability to sense the most common gases in the atmosphere such as carbon monoxide, carbon dioxide, and oxygen. This involves a pristine and doped *Gr*-sheets complex with 3 gases. Density Functional Theory (DFT), was employed to investigate the electronic structures of 12 graphene-based sheets. The bandgap simulations demonstrate the effect of doping and complexing graphene sheet with different segments, that results in a sensing signature. The bandgap calculations also prove that the studied graphene derivatives selectively bind to different gases and this characteristic is in good agreement with the total energy calculations.

**Keywords:** 2D materials, Graphene doped Ni-As, Gas sensor, DFT

## 1. Introduction

Since the first experimentally synthesised graphene (*Gr*), two-dimensional 2D materials have received a lot of attention for the creation of next-generation nanodevices. Due to its superior electrical properties involving strong carrier mobility and current density, graphene was thought to deliver good performance for nanoelectronic devices in the early stages of research on 2D materials[1-7]. Graphene nanoribbons *GNRs*, which are graphene sheets, have piqued interest in a number of research and application fields, including spintronics, catalysts, and sensors[8-12]. Pollution of the environment necessitates continuous monitoring of chosen gas concentrations, not only to maintain compliance with environmental regulations but also to protect the population's safety[13-19]. The set of hazardous gases is *CO*, *CO*<sub>2</sub>, and *O*<sub>2</sub>, which is used in various industrial and domestic applications. Carbon monoxide *CO*, carbon dioxide *CO*<sub>2</sub>, and Oxygen gases *O*<sub>2</sub>, are a colourless and odourless toxic gases (*O*<sub>2</sub> over certain limitations), *CO* is one of the major gaseous pollutants widely used in so many applications, for instance, medical use such as life support and recreational use, industrial, and scientific areas[20, 21]. Since the mid-20<sup>th</sup> century, increased emissions of carbon dioxide *CO*<sub>2</sub> and other greenhouse gases have been blamed for an increase in the earth's average near-surface air and ocean temperatures, a phenomenon known as a global warming[22-25]. However, oxygen gas can be toxic at elevated partial pressures, leading to convulsions and other health problems[26-28]. Furthermore, external materials, such as adatoms, molecules, clusters, and other foreign components, can stick to graphene's expanded surface and delocalised  $\pi$ -electron, and the substitutional doping of graphene with heteroatoms has expanded the intrinsic properties of graphene to unimaginable limits[29, 30]. Many theoretical and experimental evidence indicate the doping of graphene with different atoms like *Ni*, *As*, *N*, *B*, and *Fe* [1-3, 31-33, 29, 34, 30, 35-39, 5, 40, 41]. In this work, we are employing the first principle density functional theory (DFT) to investigate the electronic structural and other electrical properties of infinite graphene nanosheets doped with *Ni* and *As* atoms. We have also explored the adsorption of three different gases including *CO*, *CO*<sub>2</sub>, *O*<sub>2</sub>, on the graphene surface.

## 2. Methods

Graphene geometries were constructed by VMD software[42], which has an excellent capability to build 2D materials and carbon nanotubes. The distance of C-C bond is found to be 1.42 Å, which agrees well with the measured distance [43-45]. The research here is divided into three main configurations including Pristine graphene *Gr*, which contains 60 periodic carbon atoms with dimensions of 12.2 and 11.26 Å. Graphene was doped with nickel *Gr: Ni*, and graphene doped with arsenic *Gr: As*, as shown in [Supplementary Figure 1](#), and then complex three different types of gas molecules including *CO*, *CO<sub>2</sub>*, and *O<sub>2</sub>*, on the top of each type of the graphene derivatives. The graphene derivatives are all periodic in the x- and y-directions, and are isolated in the z-direction as shown in [Supplementary Figure 4](#). The optimisation of these structures was performed using density functional theory as implemented in SIESTA code[46], using generalized gradient approximation GGA, with the Perdew–Burke–Ernzerhof[47, 48] parameterisation for exchange and correlation. Double- $\zeta$  polarised basis sets applied with Monkhorst-Pack mesh  $3 \times 3 \times 1$  of *k*-point were set in Brillouin zone integration and when all forces on each atom were less than the tolerance limit 40 meV Å<sup>-1</sup>. The band structure is calculated on x-direction which is the armchair direction for all structurals in this study (for more detail see section 1 in the SI).

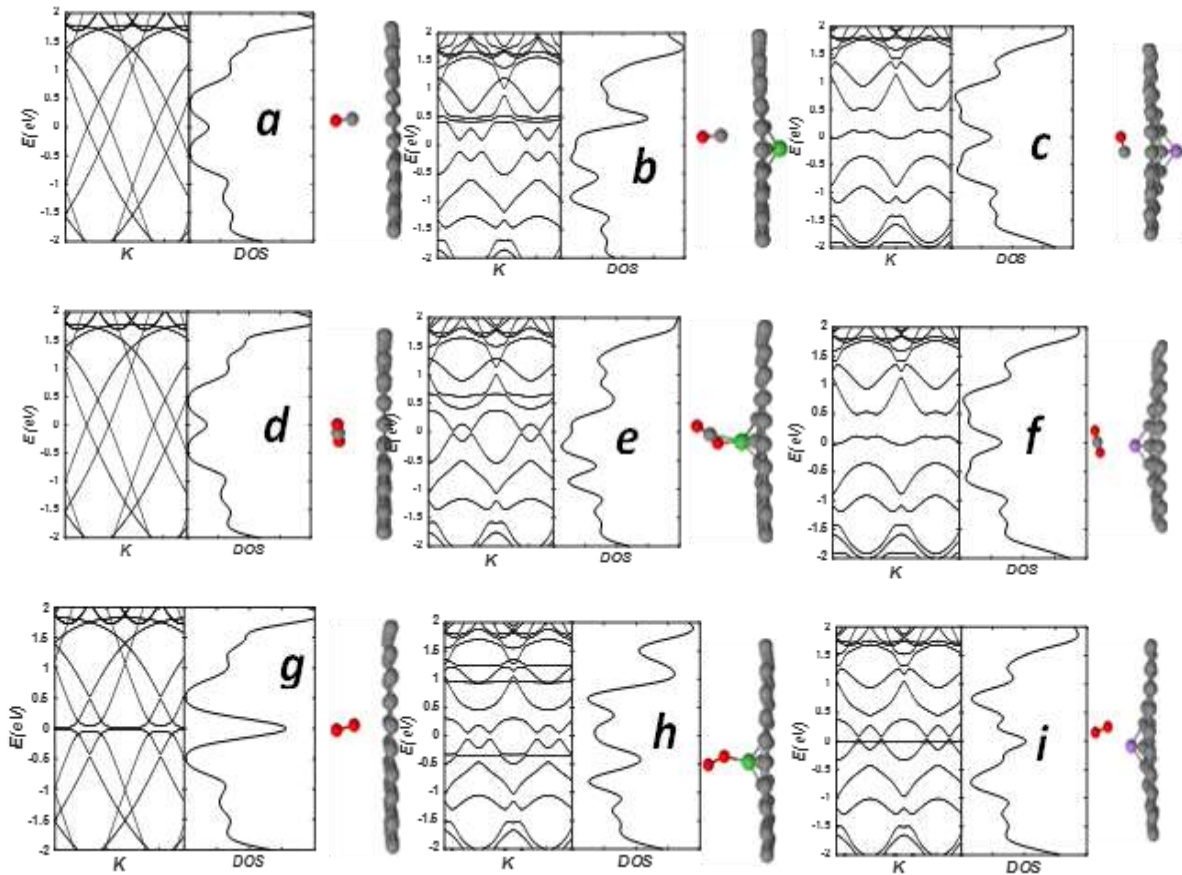
## 3. Results and Discussion

Before discussing the adsorption of *CO*, *CO<sub>2</sub>*, and *O<sub>2</sub>* gas molecules (see [Supplementary Figure 3](#)), on the graphene sheets, we consider embedding (doping) two different types of atoms such as nickel and arsenic into the pristine graphene sheets as shown in [Supplementary Figure 1b and 1c](#). The graphene-doped sheets were achieved by replacing one C atom of the Gr sheet with either a *Ni* or *As* atom ([Supplementary Figures 1b and 1c](#) respectively). [Supplementary Figure 1a](#) illustrates the periodic pristine graphene *Gr* with a uniform bond length of 1.41 Å and a flat surface. on the contrary with *Ni* and *As*, as shown in [Supplementary Figures 1b and 1c](#). The doped atoms remain almost in the same locations as the replaced C atoms, however, they squeeze the nearest three carbon atoms and change the bond lengths to become (1.70, 1.69 and 1.69) and (1.72, 1.72 and 1.71) Å between *Ni-C* and *As-C* atoms respectively. This change is attributed to the fact that the radius of *Ni* and *As* atoms are larger than that of carbon C atoms, which is  $C=0.67\text{Å}$ ,  $Ni=1.49\text{Å}$  and  $As=1.14\text{Å}$ [49]. Up to this point, we have explored the pristine graphene and two different graphene-doped sheets mainly nickel and arsenic. The next step is to complex the graphene derivatives with three gases *CO*, *CO<sub>2</sub>*, and *O<sub>2</sub>*.

[Supplementary Figure 4](#) shows the fully optimised complex geometries of *CO*, *CO<sub>2</sub>*, and *O<sub>2</sub>* gas molecules that adsorb on graphene derivatives. [Panels 4a, 4d and 4g](#) (first column), illustrate how the three gases interact with pristine graphene sheets. These panels show that both *CO* and *O<sub>2</sub>* molecules position vertically on the *Gr* sheets in hollow sites (i.e. the centre of the hexagon ring) with a small tilt angle of *O<sub>2</sub>* molecule roughly 20°. The distance between the sheet and the molecules is found to be approximately 2.7 Å for *CO* and slightly shorter for *O<sub>2</sub>* about 2.4 Å. On the other hand, *CO<sub>2</sub>* places horizontally on a bridge site (i.e. in between two atoms), of the graphene surface at a distance of approximately 2.9 Å.

The case is different with graphene-doped derivatives (i.e. in the presence of nickel and arsenic, second and third columns of [Supplementary Figure 5](#)), the behaviour here is similar to *Ni* and *As* metals. It should be noticed, that *CO* has pushed both *Ni* and *As* atoms out of the graphene

plane sheets and this displacement is in the opposite direction to the  $CO$  location. The displacement distance between  $CO$  and the doped atoms ( $Ni$  and  $As$ ), is found to be 3.82 and 3.73 Å respectively. It is worth mentioning, that  $Ni$  and  $As$  move away from  $CO$  is due to the repulsion force between  $CO$  and the doped atoms as both have similar charge types as shown in panels 1b and 1c of Fig. 1. Whereas  $CO_2$  and  $O_2$  behave differently from  $CO$ , as these molecules attract the doped atoms than repulse them. The attraction force happens here due to the fact there are different types of charges, and this leads to shortening the displacement distance. The displacement distance of  $CO_2$  and  $O_2$  with the doped atoms is as follows: 2.08, 1.78, 3.26 and 2.34 Å of  $Ni-CO_2$ ,  $Ni-O_2$ ,  $As-CO_2$  and  $As-O_2$  respectively as shown in panels 1e, 1f, 1h and 1i.



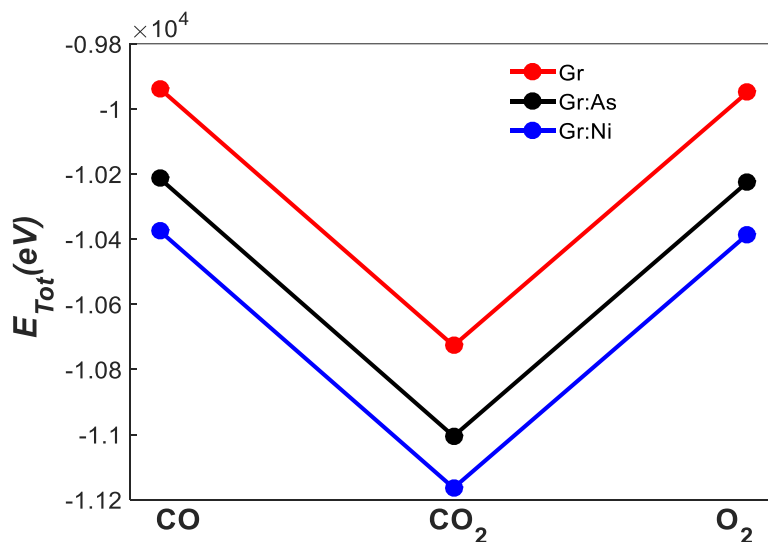
**Figure- 1:** Ground-state of optimised complex structures. First column ( $a d g$ ), pristine graphene, second column ( $b e h$ ), graphene doped- $Ni$  and third column ( $c f i$ ), graphene doped- $As$  complex with  $CO$ ,  $CO_2$ , and  $O_2$  gas molecules respectively, side view.

Fig. 1 shows the band structures and the corresponding density of states (DOS) of the pristine graphene and graphene doped complex with  $CO$ ,  $CO_2$ , and  $O_2$  gases that are adsorbed on the surface. For comparison, the band structure and DOS of  $CO$ ,  $CO_2$ , and  $O_2$  gases adsorbed on pristine graphene are plotted in Fig. 1( $a d g$ ). At the Dirac point, the pristine graphene has no bandgap as shown in Fig. 1d, at this point, the valence band and conduction band are overlapping at the Fermi level  $E_F = 0$  eV. This result is consistent with published studies[50-52].

Regarding the DOS calculations, one could easily notice the peak of graphene complex with  $O_2$  at  $E_F$  is more 3 times larger than  $CO$  and  $CO_2$  peaks at the same location as shown in the first column of Fig. 1 (panels 1a, 1d, and 1g, on the right). This significant difference is attributed to the strong interaction between the graphene sheet and the oxygen gas. In contrast, the bandgap is opened when the  $Gr: Ni$  complexes with the three gases as shown in the second column of Fig. 1 (panels 1b, 1e and 1h). This happens because the gases adsorbed on the  $Ni$ -doped sheets cause a shift in the Fermi level position towards lower energy as illustrated by the DOS curves (panels 1b, 1e and 1h, on the right). It is clearly shown that the main peaks ( $E_F = 0 eV$ ), of the  $Ni$ -doped sheets have shifted towards low energy compared to the same peaks of the pristine graphene.

The last column of Fig.1 presents the band structures of the  $As$ -doped sheets. Panels 1c, 1f, and 1i, are clearly shown that the 3 bands close up when the doped sheets complex with  $CO$ ,  $CO_2$ , and  $O_2$ . Herein, the band structure gaps are closed up is due to the  $As$  atom having 5 valence electrons, which means this atom possesses an extra free electron, whereas a  $Ni$  atom has 2 valence electrons and this explains why the gaps were opened.

Up to this point, the electronic structure of the pristine/doped graphene and complexes has been investigated, the other characters to be explored in the current study is the total energy  $E_{Total}$  of these systems. Fig.4 indicts that  $CO_2$  binds significantly stronger than  $CO$  and  $O_2$  gases to the pristine  $Gr$  (red-line), doped  $Gr:As$  (black-line), and doped  $Gr:Ni$  (blue-line). The actual difference is significant approximately 1000 eV.



**Figure- 2:** Total energy for adsorbed gas molecules on pristine graphene (red),  $Gr: Ni$  (blue), and  $Gr: As$  (black).

#### 4. Conclusion

The adsorption and reaction mechanisms of  $CO$ ,  $CO_2$ , and  $O_2$  gas molecules on a pristine  $Gr$ ,  $Ni$ - and  $As$ -doped graphene were investigated by employing the density functional method (DFT). Furthermore, the electronic structural and electrical properties were also explored for 12 graphene derivatives. The influence of complex 3 gases on pristine or doped graphene sheets is clearly demonstrated in the bandgap and DOS calculations. This influence is supported-well by the optimum distance values. The adsorption simulations suggest that the  $Gr$  derivatives interact with the 3 gases in two different ways: sensitive and insensitive, meaning these graphene-based sheets could be used as a promising gas sensor.

## References

- [1] A. A. Al-Jobory and M. D. Noori, "Electrical and thermal properties of GaAs  $1-x$  P  $x$  2D-nanostructures," *The European Physical Journal D*, vol. 73, no. 10, p. 223, 2019.
- [2] A. A. Al-Jobory, I. A. Wael, and J. J. I. J. o. S. Ibrahim, "Electronic Structure and Optical Properties of GaAs $1-x$ P $x$ : A First-Principles Study," pp. 77-82, 2020.
- [3] N. M. Al-Shareefi, A. Al-Jobory, and H. I. Abbood, "Germanene-GaAs as super media for gas sensor," in *IOP Conference Series: Materials Science and Engineering*, 2018, vol. 454, no. 1: IOP Publishing, p. 012153.
- [4] J. Cha, K.-A. Min, D. Sung, and S. J. C. A. P. Hong, "Ab initio study of adsorption behaviors of molecular adsorbates on the surface and at the edge of MoS<sub>2</sub>," vol. 18, no. 9, pp. 1013-1019, 2018.
- [5] K. S. Novoselov, A. K. Geim, S. V. Morozov, D. Jiang, Y. Zhang, S. V. Dubonos, I. V. Grigorieva, and A. A. J. s. Firsov, "Electric field effect in atomically thin carbon films," *science*, vol. 306, no. 5696, pp. 666-669, 2004.
- [6] K. S. Novoselov, D. Jiang, F. Schedin, T. Booth, V. Khotkevich, S. Morozov, and A. K. J. P. o. t. N. A. o. S. Geim, "Two-dimensional atomic crystals," vol. 102, no. 30, pp. 10451-10453, 2005.
- [7] F. J. N. n. Schwierz, "Graphene transistors," vol. 5, no. 7, p. 487, 2010.
- [8] L. Benchallal, S. Haffad, F. Boubenider, L. Lamiri, H. Zitoune, B. Kahouadji, and M. J. S. S. C. Samah, "Ab initio study of iron adatom-vacancies in armchair graphene nanoribbons," vol. 276, pp. 9-13, 2018.
- [9] J. Dorantes-Dávila and G. J. P. r. l. Pastor, "Magnetic anisotropy of one-dimensional nanostructures of transition metals," vol. 81, no. 1, p. 208, 1998.
- [10] P. Gambardella, A. Dallmeyer, K. Maiti, M. Malagoli, W. Eberhardt, K. Kern, and C. J. N. Carbone, "Ferromagnetism in one-dimensional monatomic metal chains," vol. 416, no. 6878, pp. 301-304, 2002.
- [11] A. K. Ismael, I. Grace, and C. J. Lambert, "Increasing the thermopower of crown-ether-bridged anthraquinones," *Nanoscale*, vol. 7, no. 41, pp. 17338-17342, 2015.
- [12] A. Vindigni, A. Rettori, M. Pini, C. Carbone, and P. J. A. P. A. Gambardella, "Finite-sized Heisenberg chains and magnetism of one-dimensional metal systems," vol. 82, no. 3, pp. 385-394, 2006.
- [13] T. Arakawa, X. Wang, T. Kajiro, K. Miyajima, S. Takeuchi, H. Kudo, K. Yano, K. J. S. Mitsubayashi, and A. B. Chemical, "A direct gaseous ethanol imaging system for analysis of alcohol metabolism from exhaled breath," vol. 186, pp. 27-33, 2013.
- [14] M. L. de Castro and M. J. T. T. i. A. C. Fernandez-Peralbo, "Analytical methods based on exhaled breath for early detection of lung cancer," vol. 38, pp. 13-20, 2012.
- [15] A. K. Ismael and C. J. Lambert, "Molecular-scale thermoelectricity: a worst-case scenario," *Nanoscale Horizons*, vol. 5, no. 7, pp. 1073-1080, 2020.
- [16] I. Karaduman, E. Er, H. Çelikkan, N. Erk, S. J. J. o. A. Acar, and Compounds, "Room-temperature ammonia gas sensor based on reduced graphene oxide nanocomposites decorated by Ag, Au and Pt nanoparticles," vol. 722, pp. 569-578, 2017.
- [17] A. Markin, A. K. Ismael, R. J. Davidson, D. C. Milan, R. J. Nichols, S. J. Higgins, C. J. Lambert, Y.-T. Hsu, D. S. Yufit, and A. Beeby, "Conductance Behavior of Tetraphenyl-Aza-BODIPYs," *The Journal of Physical Chemistry C*, vol. 124, no. 12, pp. 6479-6485, 2020.

- [18] J. P. Spinhirne, J. A. Koziel, and N. K. J. B. e. Chirase, "A device for non-invasive on-site sampling of cattle breath with solid-phase microextraction," vol. 84, no. 2, pp. 239-246, 2003.
- [19] X. Wang, A. Ismael, A. Almutlg, M. Alshammari, A. Al-Jobory, A. Alshehab, T. L. Bennett, L. A. Wilkinson, L. F. Cohen, and N. J. Long, "Optimised power harvesting by controlling the pressure applied to molecular junctions," *Chemical Science*, vol. 12, no. 14, pp. 5230-5235, 2021.
- [20] A. Ismael, X. Wang, T. L. Bennett, L. A. Wilkinson, B. J. Robinson, N. J. Long, L. F. Cohen, and C. J. Lambert, "Tuning the thermoelectrical properties of anthracene-based self-assembled monolayers," *Chemical science*, vol. 11, no. 26, pp. 6836-6841, 2020.
- [21] D. Zhang, C. Jiang, J. Liu, Y. J. S. Cao, and A. B. Chemical, "Carbon monoxide gas sensing at room temperature using copper oxide-decorated graphene hybrid nanocomposite prepared by layer-by-layer self-assembly," vol. 247, pp. 875-882, 2017.
- [22] A. A. Al-Jobory, Z. Y. Mijbil, and M. Noori, "Tuning electrical conductance of molecular junctions via multipath Ru-based metal complex wire," *J Indian Journal of Physics*, journal article vol. 94, pp. 1189–1194, July 15 2020, doi: 10.1007/s12648-019-01560-1.
- [23] A. Ismael, A. Al-Jobory, X. Wang, A. Alshehab, A. Almutlg, M. Alshammari, I. Grace, T. L. Benett, L. A. Wilkinson, and B. J. Robinson, "Molecular-scale thermoelectricity: as simple as 'ABC'," *Nanoscale Advances*, vol. 2, no. 11, pp. 5329-5334, 2020.
- [24] A. K. Ismael, I. Grace, and C. J. Lambert, "Connectivity dependence of Fano resonances in single molecules," *Physical Chemistry Chemical Physics*, 10.1039/C7CP00126F vol. 19, no. 9, pp. 6416-6421, 2017, doi: 10.1039/c7cp00126f.
- [25] H. J. Yoon, J. H. Yang, Z. Zhou, S. S. Yang, M. M.-C. J. S. Cheng, and A. B. Chemical, "Carbon dioxide gas sensor using a graphene sheet," vol. 157, no. 1, pp. 310-313, 2011.
- [26] M. K. Al-Khaykane, A. K. Ismael, I. Grace, and C. J. J. R. a. Lambert, "Oscillating Seebeck coefficients in  $\pi$ -stacked molecular junctions," vol. 8, no. 44, pp. 24711-24715, 2018.
- [27] C. Chen, S. Hung, M. Yang, C. Yeh, C. Wu, G. Chi, F. Ren, and S. J. A. P. L. Pearton, "Oxygen sensors made by monolayer graphene under room temperature," vol. 99, no. 24, p. 243502, 2011.
- [28] M. Sim, P. Dean, J. Kinsella, R. Black, R. Carter, and M. J. A. Hughes, "Performance of oxygen delivery devices when the breathing pattern of respiratory failure is simulated," vol. 63, no. 9, pp. 938-940, 2008.
- [29] P. A. J. C. Denis, "Chemical Reactivity and Band-Gap Opening of Graphene Doped with Gallium, Germanium, Arsenic, and Selenium Atoms," vol. 15, no. 18, pp. 3994-4000, 2014.
- [30] S. Haldar, B. S. Pujari, S. Bhandary, F. Cossu, O. Eriksson, D. G. Kanhere, and B. J. P. R. B. Sanyal, " $\text{Fe}_n$  ( $n=1-6$ ) clusters chemisorbed on vacancy defects in graphene: Stability, spin-dipole moment, and magnetic anisotropy," vol. 89, no. 20, p. 205411, 2014.
- [31] Z. Ao, J. Yang, S. Li, and Q. J. C. P. L. Jiang, "Enhancement of CO detection in Al doped graphene," vol. 461, no. 4-6, pp. 276-279, 2008.
- [32] D. Cortés-Arriagada and A. J. P. C. C. P. Toro-Labbé, "Improving As (iii) adsorption on graphene based surfaces: impact of chemical doping," vol. 17, no. 18, pp. 12056-12064, 2015.
- [33] D. Cortés-Arriagada and A. J. R. a. Toro-Labbé, "A theoretical investigation of the removal of methylated arsenic pollutants with silicon doped graphene," vol. 6, no. 34, pp. 28500-28511, 2016.
- [34] M. D. Esrafil and N. J. N. J. o. C. Saeidi, "Catalytic reduction of NO by CO molecules over Ni-doped graphene: a DFT investigation," vol. 41, no. 21, pp. 13149-13155, 2017.
- [35] N. K. Jaiswal and P. J. S. s. c. Srivastava, "Structural stability and electronic properties of Ni-doped armchair graphene nanoribbons," vol. 151, no. 20, pp. 1490-1495, 2011.

- [36] K. Jiang, S. Siahrostami, T. Zheng, Y. Hu, S. Hwang, E. Stavitski, Y. Peng, J. Dynes, M. Gangisetty, D. J. E. Su, and E. Science, "Isolated Ni single atoms in graphene nanosheets for high-performance CO<sub>2</sub> reduction," vol. 11, no. 4, pp. 893-903, 2018.
- [37] O. Leenaerts, B. Partoens, and F. J. P. R. B. Peeters, "Adsorption of H<sub>2</sub>O, NH<sub>3</sub>, CO, NO<sub>2</sub>, and NO on graphene: A first-principles study," vol. 77, no. 12, p. 125416, 2008.
- [38] R. Longo, J. Carrete, J. Ferrer, and L. J. P. R. B. Gallego, "Structural, magnetic, and electronic properties of Ni<sub>n</sub> and Fe<sub>n</sub> nanostructures (n= 1–4) adsorbed on zigzag graphene nanoribbons," vol. 81, no. 11, p. 115418, 2010.
- [39] S. Nachimuthu, P.-J. Lai, E. G. Leggesse, and J.-C. J. S. r. Jiang, "A first principles study on boron-doped graphene decorated by Ni-Ti-Mg atoms for enhanced hydrogen storage performance," vol. 5, no. 1, pp. 1-8, 2015.
- [40] E. J. Santos, A. Ayuela, S. Fagan, J. Mendes Filho, D. Azevedo, A. Souza Filho, and D. J. P. R. B. Sánchez-Portal, "Switching on magnetism in Ni-doped graphene: density functional calculations," vol. 78, no. 19, p. 195420, 2008.
- [41] E. J. Santos, A. Ayuela, and D. J. N. J. o. P. Sánchez-Portal, "First-principles study of substitutional metal impurities in graphene: structural, electronic and magnetic properties," vol. 12, no. 5, p. 053012, 2010.
- [42] W. Humphrey, A. Dalke, and K. Schulten, "VMD: visual molecular dynamics," *Journal of molecular graphics*, vol. 14, no. 1, pp. 33-38, 1996.
- [43] R. J. Davidson, D. C. Milan, O. A. Al-Owaedi, A. K. Ismael, R. J. Nichols, S. J. Higgins, C. J. Lambert, D. S. Yufit, and A. Beeby, "Conductance of 'bare-bones' tripod molecular wires," *RSC advances*, vol. 8, no. 42, pp. 23585-23590, 2018.
- [44] L. Herrero, A. Ismael, S. Martín, D. C. Milan, J. L. Serrano, R. J. Nichols, C. Lambert, and P. Cea, "Single molecule vs. large area design of molecular electronic devices incorporating an efficient 2-aminepyridine double anchoring group," *Nanoscale*, vol. 11, no. 34, pp. 15871-15880, 2019.
- [45] S. Naghibi, A. K. Ismael, A. Vezzoli, M. K. Al-Khaykanee, X. Zheng, I. M. Grace, D. Bethell, S. J. Higgins, C. J. Lambert, and R. J. Nichols, "Synthetic Control of Quantum Interference by Regulating Charge on a Single Atom in Heteroaromatic Molecular Junctions," *The journal of physical chemistry letters*, vol. 10, no. 20, pp. 6419-6424, 2019.
- [46] J. M. Soler, E. Artacho, J. D. Gale, A. García, J. Junquera, P. Ordejón, and D. J. J. o. P. C. M. Sánchez-Portal, "The SIESTA method for ab initio order-N materials simulation," *Journal of Physics: Condensed Matter*, vol. 14, no. 11, p. 2745, 2002.
- [47] B. Hammer, L. B. Hansen, and J. K. J. P. r. B. Nørskov, "Improved adsorption energetics within density-functional theory using revised Perdew-Burke-Ernzerhof functionals," vol. 59, no. 11, p. 7413, 1999.
- [48] J. P. Perdew, K. Burke, and M. J. E. P. R. L. Ernzerhof, "Phys rev lett 77: 3865," vol. 78, p. 1396, 1996.
- [49] E. Clementi and D.-L. Raimondi, "Atomic screening constants from SCF functions," *The Journal of Chemical Physics*, vol. 38, no. 11, pp. 2686-2689, 1963.
- [50] M. Goudarzi, S. Parhizgar, and J. J. J. o. E. M. Beheshtian, "Ab Initio Study of Mono-Layer Graphene as an Electronical or Optical Sensor for Detecting B, N, O and F Atoms," *Journal of Electronic Materials*, vol. 48, no. 7, pp. 4265-4272, 2019.
- [51] M. Omid and E. J. J. o. A. P. Faizabadi, "Edge deformation effects on sensitivity and selectivity performance of graphene quantum ring gas sensor," *Journal of Applied Physics*, vol. 125, no. 17, p. 174503, 2019.
- [52] N. Tit, K. Said, N. M. Mahmoud, S. Kouser, and Z. H. J. A. S. S. Yamani, "Ab-initio investigation of adsorption of CO and CO<sub>2</sub> molecules on graphene: Role of intrinsic defects on gas sensing," *Applied Surface Science*, vol. 394, pp. 219-230, 2017.